

Conductance distributions of 1D-disordered wires at finite temperature and bias voltage.

Federico Foieri

*Departamento de Física “J. J. Giambiagi” FCEyN, Universidad de Buenos Aires,
Ciudad Universitaria Pab.I, (1428) Buenos Aires, Argentina*

María José Sánchez

Centro Atómico Bariloche and Instituto Balseiro, Bustillo 9500 (8400), Bariloche, Argentina

Liliana Arrachea

*Departamento de Física de la Materia Condensada, and
Instituto de Biocomputación y Física de Sistemas Complejos,
Universidad de Zaragoza, Corona de Aragón 42, 50009 Zaragoza, Spain*

Victor A. Gopar

*Instituto de Biocomputación y Física de Sistemas Complejos,
Universidad de Zaragoza, Corona de Aragón 42, 50009 Zaragoza, Spain*

We calculate the distribution of the conductance G in a one-dimensional disordered wire at finite temperature T and bias voltage V in an independent-electron picture and assuming full coherent transport. At high enough temperature and bias voltage, where several resonances of the system contribute to the conductance, the distribution $P(G(T, V))$ can be represented with good accuracy by autoconvolutions of the distribution of the conductance at zero temperature and zero bias voltage. The number of convolutions depends on T and V . In the regime of very low T and V , where only one resonance is relevant to $G(T, V)$, the conductance distribution is analyzed by a resonant tunneling conductance model. Strong effects of finite T and V on the conductance distribution are observed and well described by our theoretical analysis, as we verify by performing a number of numerical simulations of a one-dimensional disordered wire at different temperatures, voltages, and lengths of the wire. Analytical estimates for the first moments of $P(G(T, V))$ at high temperature and bias voltage are also provided.

PACS numbers: 72.10.-d, 73.23.-b, 72.15.Rn

I. INTRODUCTION

The continuous progress in the fabrication of small electronic circuits has kept active the theoretical study of quantum electronic transport. For example, transport properties in point contacts, atomic chains, carbon nanotubes, and quantum wires are currently under experimental investigations^{1,2,3,4,5,6}. Although the theoretical study of electronic transport in mesoscopic systems—where the phase coherence of electrons is preserved along the whole device—has been of great interest for several decades, these recent experimental advances have further renewed the motivation of theoreticians for studying the electronic transport through one-dimensional structures.

In a disordered mesoscopic wire the random position of impurities gives a stochastic character to the electronic transport. Therefore, it is of particular relevance the analysis of the statistical properties of transport quantities like the conductance. On the theoretical side, there is a full description of the statistical properties of the conductance in quasi-one-dimensional disordered systems within an independent-electron picture at zero temperature T and “zero bias” (actually, infinitesimally small voltage) V .^{7,8} This degree of detail in the theoretical description is, however, not available for disordered wires at

finite temperatures and bias voltage, even in the simple case of one-dimensional (1D) wires. This is an unfortunate fact since experiments are usually performed within a wide range of T and V . For example, the effect of finite bias voltage has been found to modify the behavior of the conductance fluctuations.^{4,5,6}

Several efforts have been made in order to incorporate the information of a finite T into the statistical description of quantum electronic transport in 1D-disordered systems. In Ref. 9, at zero voltage, a model of zero-width resonances represented by δ -functions was introduced in order to calculate the dependence on the temperature of the averages of the conductance $\langle G(T) \rangle$ and $\langle \ln G(T) \rangle$. Assuming full coherent transport, in Ref. 10 the effect of the thermal smearing on the mean resistance of a 1D wire was studied.

At finite temperature and bias voltage, the distribution of the conductance $P(G(T, V))$ was calculated in Ref. 11 by using a statistical model of resonant tunneling transmission. The methodology there employed was, however, restricted to disordered wires of length $L \gg l$, where l is the mean free path, and very small values of T and V (although sizable): typically eV and kT were considered of the order or smaller than the mean spacing between energy levels Δ . Within this regime of temperatures and

voltages it can be assumed that only one resonance—the closest to the Fermi energy—contributes to the transport. Even with these limitations, that work shows that the conductance distribution do display novel features as a consequence of finite T and V values. Particularly, it was shown that the distribution of conductances narrows as the value of T and/or V is increased.

We would like to remark that the assumption of phase coherent transport adopted in previous works, as well as in the present one, is restricted by the phase relaxation L_ϕ at finite temperature and voltage. For example, inelastic scattering and thermally activated hopping processes,^{12,13,14} which might be important at finite values of T , V are not considered in our analysis. In Ref. 11, however, it is discussed the possibility of satisfying $L_\phi > L$ even at finite temperature and bias voltage for short enough wires, which opens the possibility of observing the effect of finite T, V on the statistical properties of the conductance in realistic systems. It is also interesting to note that the range of voltage V where the averaged charge current $\langle J(T, V) \rangle$ is a linear function of V or departs slightly from this behavior, i.e., the so-called *linear response* regime, can be rather wide as we will show in Section III.

The main goal of the present paper is to compute the distribution of the conductance $G(T, V)$ at values of eV and kT typically larger than the mean level spacing, where several resonances contribute to the conductance. We show that, within this regime of temperatures and voltages, the distribution of the conductance can be well described in terms of the convolutions of the zero temperature/voltage conductance distribution $p(g)$. The number of distributions to be convolved is determined by the number of resonances in an energy window where electron transport can take place. This energy window is defined by the value of the temperature and voltage. The method introduced in the present work applies to any degree of disorder i.e. *to any value* of the ratio L/l , provided several resonances contribute to the transport, allowing for the investigation of short wires where coherent transport is more likely to be observed. For completeness in the sense that all regimes of temperature and voltage will be covered in this paper, we also study the regime of small T and V following Ref. 11

This paper is organized as follows. In Sec. II we present the methodology to analytically calculate the conductance distribution $P(G(T, V))$. We divide this section into two subsections. The first one, II A, is devoted to review the case of small temperatures and voltage regimes where one can assume that only the closest resonance to the Fermi energy contribute to the conductance.¹¹ In the second one, subsection II B, we introduce a method based on the convolution of the known distribution of conductances at zero temperature and bias voltage in order to study the regime of high temperatures and bias voltages.

In section III we present the model used in our simulations and show some general features of our 1D-

disordered system obtained numerically, which support the assumptions introduced in our theoretical proposal of section II. In section III we also compare the results of the distribution $P(G(T, V))$ from the numerical simulations to the predictions of the theoretical approach presented in the previous section, for the different regimes of T and V . Finally, in section IV we give a summary and conclusions of our study of the distribution of conductances at finite temperature and bias voltage.

II. METHODOLOGY

We consider the usual setup where the disordered conductor is placed between left and right reservoirs at the same finite temperature T and chemical potentials $\mu_L = \mu + eV/2$ and $\mu_R = \mu - eV/2$, respectively. The conductance $G(T, V) = J(T, V)/eV$ can be written as (in units of the conductance quantum $2e^2/h$)

$$G(T, V) = \frac{1}{eV} \int_{-\infty}^{\infty} dE g(E) (f(E - eV/2, T) - f(E + eV/2, T)), \quad (1)$$

where $f(E, T) = \{\exp[(E - \mu)/kT] + 1\}^{-1}$ is the Fermi function, being k the Boltzmann constant, while $g(E)$ is the dimensionless conductance for $E = \mu$ at $T = 0$. It is clear from the above integral expression for $G(T, V)$ that the energy window where electronic transport takes place will depend on the values of T and V . This can be emphasized recasting the difference in the Fermi functions in the above expression, Eq.(1), as¹⁵

$$f(E - eV/2, T) - f(E + eV/2, T) = (\Theta(E - eV/2) - \Theta(E + eV/2)) * \frac{-\partial f(E, T)}{\partial E}, \quad (2)$$

where the symbol $*$ denotes the convolution in energy, $\Theta(x)$ is the unit step function, and $\partial f(E, T)/\partial E$ is the thermal smearing function. Therefore, the difference of the Fermi functions can be expressed as a convolution in energy of two functions: one depends only on the applied voltage V and the other one, only on temperature T . This implies that thermal and voltages effects are statistically independent, and this will be useful to calculate the distribution of $G(T, V)$.

A. Small temperatures and bias voltages: one-resonance contribution to $G(T, V)$

In this subsection we briefly review the resonant model introduced in Ref. 11. This model is appropriate for systems with non overlapping resonances, which is satisfied for disordered systems with $L > l$. Assuming a Lorentzian line shape for the resonances, the dimensionless conductance $g(E)$ at $T = 0, V \sim 0$ can be written as^{11,16}

$$g(E) = \sum_{\nu} \frac{\Gamma_{\nu}^{(l)} \Gamma_{\nu}^{(r)}}{(E - E_{\nu})^2 + \Gamma_{\nu}^2/4}, \quad (3)$$

where $\Gamma_\nu = \Gamma_\nu^{(\ell)} + \Gamma_\nu^{(r)}$ is the total width, $\Gamma_\nu^{(\ell,r)} \propto \Delta \exp[-(L \pm 2z_\nu)/\xi_\nu]$ are the left and right partial widths, and ξ_ν are the localization lengths. On resonance ($E = E_\nu$), the terms of the sum Eq. (3), $t_\nu = [\cosh(2z_\nu/\xi_\nu)]^{-2}$, depend on the location z_ν of the state, and are maximum for $z_\nu = 0$ (center of wire). Substituting Eq. (3) into Eq. (1), it is found that the conductance $G(T, V)$ is given by

$$G = -2\pi kT \text{Re} \left[\sum_\nu \sum_{n=0}^{\infty} \frac{t_\nu \Gamma_\nu}{(E_\nu - \mu + i\Gamma_\nu + i\omega_n)^2 - (eV/2)^2} \right], \quad (4)$$

where $w_n = (2n+1)\pi kT$. We now assume that $\Gamma_\nu \ll kT$, $eV \lesssim \Delta$. Under this condition only the resonance closest to the Fermi level ($\nu = 0$) contributes to the conductance $G(T, V)$ and therefore Eq. (3) can be simplified to¹¹

$$G(T, V) = \frac{\pi t_0 \Gamma_0}{2 eV} \times \left[\tanh\left(\frac{E_0 - \mu - eV/2}{2kT}\right) - \tanh\left(\frac{E_0 - \mu + eV/2}{2kT}\right) \right]. \quad (5)$$

In order to calculate the distribution of the conductance $P(G(T, V))$ a statistical model for the resonances is introduced: the resonances E_0 and their positions z_0 are considered uniformly distributed in a interval Δ and L , respectively, while the distribution of the inverse of the localization lengths $p(x_0 = 2L/\xi_0)$ follows a Gaussian distribution with mean $\langle x_0 \rangle = L/l$ and $\text{var}(x_0) = 2\langle x_0 \rangle$. This distribution for $p(x_0)$ is good for systems with $l \ll L$. In Section III we will show some examples for the distribution $P(G(T, V))$ obtained within this resonant tunneling model.

B. Large temperatures and bias voltages: contribution from several resonances to $G(T, V)$

We now go to the main goal of this work and propose a description of the conductance distribution, which is valid for arbitrary length of the wire and for voltages and temperatures satisfying $eV, kT > \Delta$, but small enough to satisfy that the behavior of the average current does not depart from linear response.

Firstly, we discretize the integral in Eq. (1) as

$$G(T, V) \approx \frac{\delta E}{eV} \sum_{i=1}^{\infty} g(E_i) [f(E_i - (\mu - eV/2), T) - f(E_i - (\mu + eV/2), T)], \quad (6)$$

where we have assumed the same width δE for all the elements in the sum, Eq. (6).

1. Zero temperature, finite bias voltage

Let us first consider the simple case of finite bias voltage and zero temperature. In this case, the thermal broadening function in Eq. (2) is a delta function and therefore $g(E)$ in Eq. (1) is only multiplied by a rectangular function of width eV . Thus Eq. (6) is reduced to

$$G(T = 0, V) \approx \frac{1}{N} \sum_{i=1}^N g(E_i), \quad (7)$$

where the number of terms in the sum N satisfies $N\delta E = eV$. This approximation is exact in the limit $N \rightarrow \infty$. However, being our aim the evaluation of $P(G(T, V))$, we approximate (7) by a finite number N of *statistically independent* contributions. We now assume that this number corresponds to the mean number of levels in an energy window eV , i.e., $N = eV/\Delta$. This is a natural assumption since for a given disorder realization $g(E)$ is a spectral function with peaks at the energy levels of the wire (resonances). In a non-interacting electron picture, the height of the resonance peaks, as well as the energy levels change for different disorder realizations, but the average separation between levels is a well defined quantity and the spectral weights centered at the different energy levels are uncorrelated. In addition, we assume that $g(E)$ is a random stationary function of the energy, at least in the energy window where transport takes place. Then the statistical properties of $g(E)$ do not change in such energy window and therefore the distributions $p(g(E_i))$ are actually independent of the energy E_i , i.e. $p(g(E_i)) \equiv p(g)$.

Under the above assumptions the distribution $P(G(T = 0, V))$ can be computed from the convolution of N distributions $p(g)$, i.e., the N th autoconvolution of the distribution at zero temperature and bias voltage:

$$P(G(T = 0, V)) = p^{(1)}(\hat{g}) * p^{(2)}(\hat{g}) * \dots * p^{(N)}(\hat{g}), \quad (8)$$

where we have defined $\hat{g} \equiv g/N$, and the upper indices enumerate the number of distributions $p(g)$ that enters into the convolution.

As we mentioned in the Introduction, at zero temperature and infinitesimal small bias voltage the statistical properties of the transport quantities, in particular the distribution $p(g)$ for 1D and quasi-1D disordered systems is well known. In a framework of random-matrix theory, a diffusion equation known as Dorokhov-Mello-Pereyra-Kumar (DMPK) equation has been successful in describing the evolution of the conductance distribution $p(g)$ as a function of the system length L in quasi-one dimensional systems⁷. For strictly 1D wires the DMPK equation is reduced to the Melnikov equation whose solution $p(g)$ can be written as⁸

$$p(g) = \frac{1}{\sqrt{2\pi}} \left(\frac{1}{s}\right)^{\frac{3}{2}} \frac{e^{-s/4}}{g^2} \int_{y_0}^{\infty} dy \frac{ye^{-y^2/4s}}{\sqrt{\cosh y + 1 - 2/g}}, \quad (9)$$

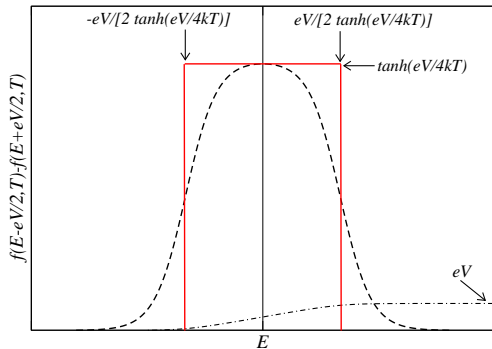


FIG. 1: (Color online) Sketch of the behavior of the function (13) and its approximation by a rectangular function, in black dashed and red solid lines. The behavior of the integral of the function (13) is also indicated in dashed-dotted lines.

where $y_0 = \text{arccosh}(2/g - 1)$ and $s = L/l$ is the length of the system L in units of the mean free path l . In the limit of $s \gg 1$ and $s \ll 1$ closed analytical expressions for $p(g)$ can be obtained.^{8,17} We remark that the only parameter that enters in the distribution $p(g)$ is the so-called disorder parameter $s = L/l$.

The simple relationship between the random variables $G(T = 0, V)$ and g , Eq. (7), encloses important conclusions since this means that the Cumulant Generating function for G and \hat{g} are also simple related:

$$\log M_G(\Lambda) = N \log (M_{\hat{g}}(\Lambda)) , \quad (10)$$

with $M_\gamma(\Lambda) \equiv \int \exp(-\Lambda\gamma) P(\gamma) d\gamma$ being $\gamma = G, \hat{g}$, while for the average and the first three central moments $\Sigma_q \equiv \langle (G - \langle G \rangle)^q \rangle$ and $\sigma_q = \langle (g - \langle g \rangle)^q \rangle$ it is satisfied:

$$\langle G \rangle = \langle g \rangle , \quad (11)$$

$$\Sigma_q = \frac{1}{N^{(q-1)}} \sigma_q \quad \text{for } q = 2, 3 . \quad (12)$$

$\sigma_1 = 0$ by definition. Then, Eq.(11) shows that the mean value of the conductance $\langle G \rangle$ is independent of the bias voltage V .

2. Finite temperature and bias voltage

Let us now consider a more realistic situation where temperature and bias voltage are both finite.

At finite temperature, the difference of Fermi functions in Eq. (1) reads

$$f(E - (\mu - eV/2), T) - f(E - (\mu + eV/2), T) = \frac{1}{2} \left[\tanh \left(\frac{E - (\mu - eV/2)}{2kT} \right) - \tanh \left(\frac{E - (\mu + eV/2)}{2kT} \right) \right]. \quad (13)$$

In fig. 1 it is shown the behavior of Eq. (13). In order to keep our statistical analysis of the conductance as simple

as possible, we approximate the bell-shaped function (13) by a rectangular function of height of $\tanh(eV/4kT)$ and width $eV/\tanh(eV/4kT)$. The area of the rectangle is, therefore, eV as the area of the original bell-shaped function Eq. (13). This simplification allows us to proceed as in subsection II B 1: from the width $eV/\tanh(eV/4kT)$ we define an “effective number of resonances”, N_{eff} , given by

$$N_{eff} = \frac{eV}{\Delta \tanh(eV/4kT)}. \quad (14)$$

We can verify that for $T \rightarrow 0$, $N_{eff} \rightarrow N = eV/\Delta$, as expected. Thus to calculate $P(G(T, V))$ we can follow exactly the same procedure of the previous subsection II B 1, we just replace N by N_{eff} . Also, at finite T and V it is possible to define a simple relation between cumulants and moments of the distribution $P(G(T, V))$ and $p(g)$; again, substituting N by N_{eff} in Eq. (12).

III. NUMERICAL RESULTS

In this section we verify our theoretical study of the statistical properties of the conductance, in particular the conductance distribution, by comparing to numerical simulations of a 1D-disordered wire. The results presented here give numerical evidence that supports the main hypothesis of our theoretical model and benchmark the quality of the approximation of the distribution function at finite bias and temperature on the basis of convolutions of the distribution in Eq. (9) against exact numerical results.

In our simulations we model a 1D-disordered wire of length L using the

standard tight binding Hamiltonian of spinless electrons with a single atomic orbital per lattice site and nearest neighbors hopping parameter t :

$$H^{wire} = -t \sum_{j=1}^{N_s} (c_j^\dagger c_{j+1} + H.c.) + \sum_{j=1}^{N_s} \varepsilon_j c_j^\dagger c_j, \quad (15)$$

with $L = N_s a$, being a the lattice constant, which we set as the unit of length and N_s , the number of sites of the 1D lattice. The on site energies ε_j are chosen randomly from an uniform distribution of width W (Anderson model). All the energy scales are taken dimensionless in units of the hopping parameter t . The disordered conductor is connected to the left and to the right to 1D clean semi-infinite leads, which we assume to be at chemical potentials $\mu_L = \mu + eV/2$ and $\mu_R = \mu - eV/2$, respectively, and temperature T . The Hamiltonian describing the contacts between the reservoirs and the disordered wire reads:

$$H^{cont} = -t(c_1^\dagger c_{k_L} + c_{N_s}^\dagger c_{k_R} + H.c.), \quad (16)$$

being $k_{L,R}$ the contact sites of the left and right semi-infinite leads, respectively.

For each disorder realization, the current is numerically calculated from the expression (1), with

$$g(E) = \Gamma^2(E) |G_{1N_s}^R(E)|^2, \quad (17)$$

being $\Gamma(E) = |t|^2 \Theta(|E| - 4t) \sqrt{16t^2 - E^2} / 4t^2$, which corresponds to reservoirs modeled by semi-infinite tight-binding chains with hopping t , while $G_{1N_s}^R(E)$ is the retarded Green's function for the disordered chain connected to the reservoirs.¹⁸ Typically, we generate numerically 10^4 to 10^5 realizations of disorder. For several values of the disorder parameter $s = L/l$, we have verified that for very small bias ($eV \ll \Delta$) and $T = 0$ we are able to reproduce the distribution $p(g)$ given by Eq. (9). The mean free path l is extracted from the numerical simulations through the relation $\langle \ln g \rangle \equiv -L/l$. In all numerical simulations we present below we have fixed $\mu = 0$ and the disorder strength to $W = 0.5$ which sets $l = 144$.

The theoretical distributions $P(G(T, V))$, as described by Eq. (8) of the previous section, are obtained by collecting the data for $G(T, V)$ from an ensemble of conductances generated numerically using a Metropolis Monte Carlo algorithm.

A. General features

Before presenting our results for the probability distribution at finite temperature and bias voltage, we would like to establish the range of the bias voltage V where the averaged current $\langle J(T = 0, V) \rangle$ varies linearly with V . To this end we have included in Eq. (15) the potential drop due to the presence of the bias by modifying the local energies as $\varepsilon_j \rightarrow \varepsilon_j + eV/2 - jeV/N_s$. In Fig. 2 we show the disorder averaged current $\langle J(T, V) \rangle$ as a function of the bias voltage, at $T = 0$. A linear behavior of $\langle J(V) \rangle$ with the bias V is observed up to $V \lesssim 0.5$ for different lengths of the system. Therefore if we want to restrict our study to the linear response regime, we cannot take arbitrary large values of T and V . In the present model, this implies energy values for eV and $kT \lesssim 0.5$. Let us note, that this range of energy is actually rather wide: it is larger than 10% of the total band width of the clean system (equal to $4t$). Since we focus in voltages within the linear response regime, in what follows we consider the wire model (Eq. (15)) without including the effect of the potential drop in the local energies ε_j .

In the inset of Fig. 2 we also show the average of the conductance $\langle G(T, V) \rangle$ for different values of T , V , as a function of the system length L . We observe that $\langle G(T, V) \rangle$ is independent of the values of the temperature and voltage and decreases exponentially with L as it is expected. This behavior is in agreement with previous results¹¹ as well as with the prediction based on Eq. (11).

Another important point to verify is the reliability of our assumption that the mean energy spacing between levels of Eq.(15) sets the energy scale

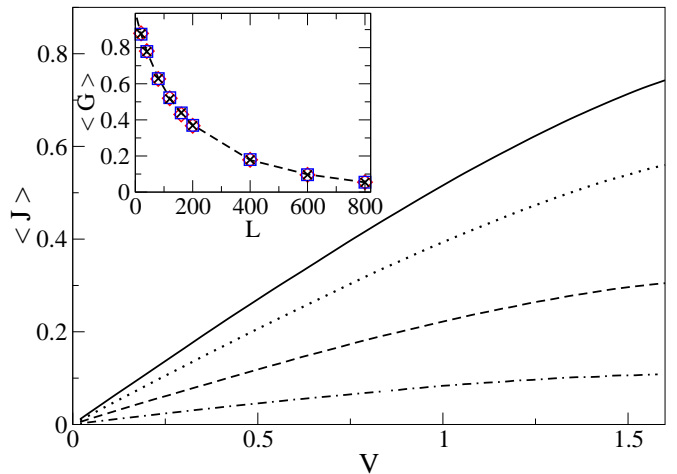


FIG. 2: (Color online) $\langle J(T, V) \rangle$ as a function of V for $W = 0.5$, $\mu = 0$ and different lengths $L = 120$ (solid), $L = 200$ (dotted), $L = 400$ (dashed), and $L = 800$ (dashed-dotted). Inset: $\langle G(T, V) \rangle$ vs L for $T = 0$ and $V = 0.01$ (black crosses), $V = 0.1$ (blue squares) and $V = 0.2$ (red diamonds). Note that the different symbols are overlapped.

where the spectral weights of $g(E)$ are statistically independent. To this end, we have investigated the behavior of the auto-correlation function $C(\varepsilon) \equiv \overline{\langle g(E)g(E + \varepsilon) \rangle} - \langle g(E) \rangle \langle g(E + \varepsilon) \rangle$, where the over line means energy average. In Fig. 3 we have plotted $C(\varepsilon)$ (normalized by dividing by $C(0)$) for three different wire lengths: $L = 40, 120$ and 800 . In all the cases $C(\varepsilon)$ decays between 90% \sim 99% of its value at $\varepsilon = 0$ for $\varepsilon < \Delta$. In order words, $C(\varepsilon)$ is a vanishing function in an energy scale ε smaller than the mean level spacing.

We have also verified numerically that in the linear response regime $p(g(E))$ is in fact independent of E , as we assumed in the previous section.

On the other hand, it is instructive to show the evolution of the conductance distribution $P(G(T, V))$ with the number of autoconvolutions of $p(g)$, as described in the previous section. We have chosen the simple case of $T = 0$ with and finite $V = 0.1$ with $s = 400/144 \approx 2.7$. In Fig. 4, the histogram in dashed line corresponds to the distribution obtained from our numerical simulations, while the histograms in solid line correspond to $P(G)$ obtained by m autoconvolutions of $p(g)$, for $m = 4, 6, 8$, and 10 . We can observe that as m increases from 4 to 6 the theoretical $P(G)$ evolves to the numerical distribution. When $m = N = 8$, which corresponds to the mean number of levels N for $L = 400$, see Fig. 3, a very good agreement is found with the numerical distribution. The fact that the optimum number of autoconvolutions of $p(g)$ coincides at $T = 0$ with the mean number of levels within eV , supports the validity of our approach of subsection II B 1.

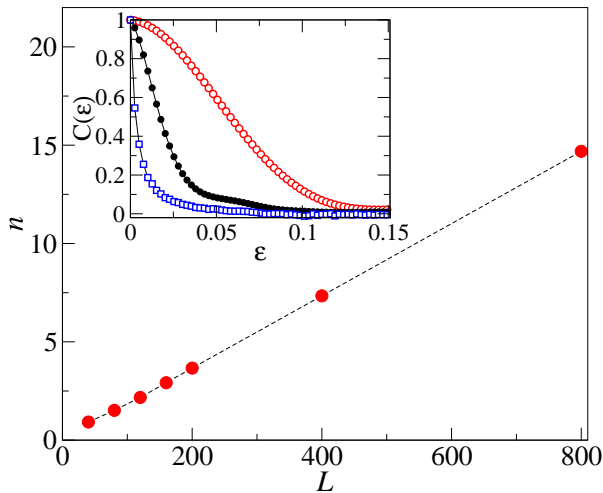


FIG. 3: (Color online) Mean number of levels n of the Hamiltonian (15) in an energy interval equal to 0.1, as a function of the system length L . Inset: The autocorrelation function $C(\epsilon)$ is plotted for $L = 40$, ($\Delta = 0.108$), $L = 120$, ($\Delta = 0.046$) and $L = 800$, ($\Delta = 0.007$) (red open circles, black solid circles and blue square symbols, respectively). See the text for details.

B. Small temperatures and bias voltage: $P(G(T, V))$ from one resonance contribution to $G(T, V)$

In this subsection we show some numerical results for the distribution $P(G)$ when the values of the temperature and bias voltage are small enough that only one resonance contributes to the conductance $G(T, V)$ (subsection II A). We also indicate the limitations of this method by showing an example of the conductance distribution at regimes of T and V beyond the scope of the resonant model.

The theoretical distribution $P(G(T, V))$ is calculated by generating numerically an ensemble of conductances G accordingly to Eq. (5), where the random variables E_0 and z_0 are obtained numerically from a uniform distribution, while x_0 is extracted from a Gaussian distribution, as it is described in II A.

In figure 5 we show the distribution of $\ln G$ (we have chosen the variable $\ln G$ since the details of the distribution can be better seen in the logarithm scale) from the resonant tunneling model (histogram in solid line) for the case of $L = 400 \sim 3l$ and $eV = \Delta$. A good agreement with the numerical simulation (histogram in dashed line) is seen. Note that, although this situation corresponds to a small bias voltage, the exact distribution (solid lines) clearly departs from the behavior of the “zero” bias distribution $p(g)$ (histogram in dotted lines). Therefore the resonant model reasonably describes the numerical behavior of $P(G)$, in particular the decrease of the width of the distribution as V, T increases (with $V, T < \Delta$). How-

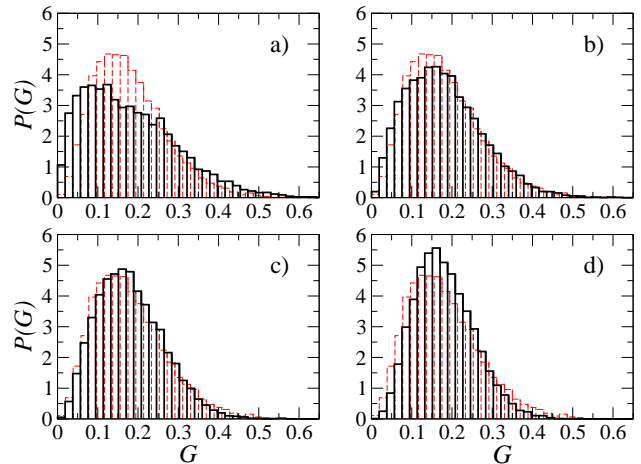


FIG. 4: (Color online) Histograms obtained from Eq.(8) performing different number of convolutions m , for a finite voltage $V = 0.1$ and $L = 400$. a) $m = 4$, b) $m = 6$, c) $m = 8$ and d) $m = 10$. For comparison the distribution $P(G)$ (histogram in red dashed line) obtained numerically is also plotted. For $m = 8$ ($= N$) convolutions the distribution $P(G)$ is quite well reproduced. The size bins of the numerical and theoretical histograms are slightly different to distinguish better

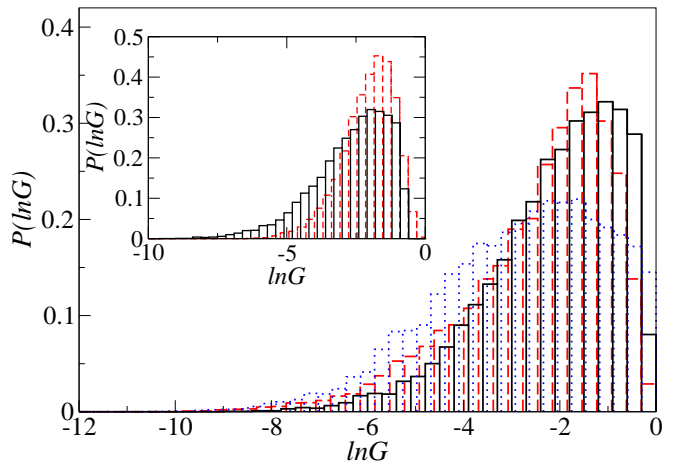


FIG. 5: (Color online) Histograms obtained with the resonant model of subsection II A (solid black lines) for $L = 400$. Results in dashed red lines correspond to the numerical simulations on the disordered tight-binding chain. Plots in the main panel correspond to $V = \Delta, T = 0$ while the inset corresponds to $V = \Delta, T = \Delta/3$. The distribution $p(g)$ is also shown in the main panel (blue dotted line).

ever, if we increase the value of T , keeping $eV = \Delta$, in our previous numerical example, the quality of the approximation provided by this model deteriorates, as it is illustrated in the inset of the figure 5. This happens in general when the values T and/or V are increased in such a way that more than one resonance might contribute to the conductance. In the next subsection we will see that

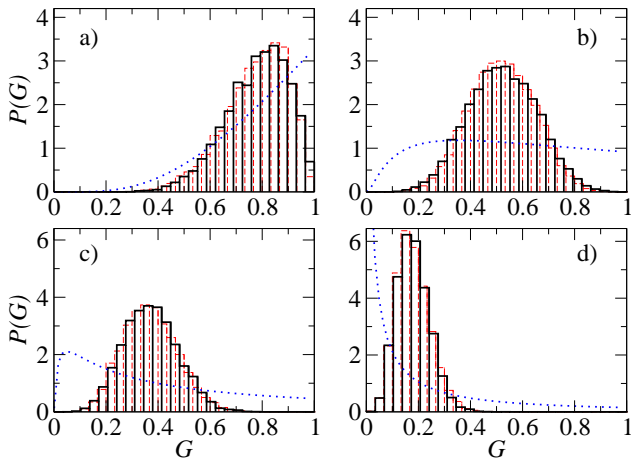


FIG. 6: (Color online) Distributions $P(G)$ for $V = 0.2$ and $T = 0$ (red dashed line histogram) obtained numerically for different lengths a) $L = 40$, b) $L = 120$, c) $L = 200$, and d) $L = 400$. The solid black line histograms correspond to the distribution of G obtained as a convolution of N terms a) $N = 2$, b) $N = 4$, c) $N = 7$, d) $N = 14$. The blue dotted curves show $p(g)$ for zero bias and temperature. The size of the bins of the numerical and theoretical histograms are slightly different to distinguish better between both histograms.

the convolution method describe correctly the regime of T and V when several resonances are involved in the transport problem.

C. Large temperature and bias voltage: $P(G(T, V))$ from several resonances contributions to $G(T, V)$

1. Zero temperature and finite bias voltage

Let us now go to the analysis of the probability distribution function at finite V with $T = 0$ using the methodology introduced in subsection II B 1. In figure 6 we show the distributions $P(G(T = 0, V))$ for different lengths L of the disordered wire with $V = 0.2$. We recall that $l = 144$ in all cases. For each length L , the distribution $P(G)$ obtained from Eq.(8) (histogram in solid line) and the numerical distribution (histogram in dashed line) are both displayed for their comparison. A very good agreement can be seen. In order to provide evidence of the strong effect of the finite bias voltage on the conductance distribution, $p(g)$ is also shown in dotted lines in the same figure.

We have also verified the relation between the second and third moments, Eq. (12). For a bias voltage $V = 0.2$, in Table I we show the values of Σ_q extracted from the numerical simulation and those for σ_q ($T = V = 0$) calculated from then integral expression of $p(g)$, Eq. (9). Again, a good agreement between numerics and theory is obtained.

TABLE I: moments Σ_q ($q = 2, 3$) for bias voltage $V = 0.2$, $W = 0.5$ for different lengths L obtained numerically and σ_q from the distribution $p(g)$, Eq.(9).

L	N	Σ_2 $\times 10^{-2}$	σ_2/N $\times 10^{-2}$	Σ_3 $\times 10^{-3}$	σ_3/N^2 $\times 10^{-3}$
40	2	1.469	1.427	-1.32	-1.01
80	3	1.716	1.802	-0.574	-0.460
120	4	1.554	1.733	0.010	0.054
200	7	1.099	0.933	0.32	0.263
400	14	0.414	0.383	0.160	0.110
800	29	0.065	0.071	0.015	0.012

TABLE II: Moments Σ_q ($q = 2, 3$) for bias voltage $V = 0.01$, $W = 0.5$ and several temperatures T for $L = 400$ obtained numerically and σ_q from the distribution $p(g)$, Eq.(9) .

T	N_{eff}	Σ_2 $\times 10^{-2}$	σ_2/N_{eff} $\times 10^{-2}$	Σ_3 $\times 10^{-3}$	σ_3/N_{eff}^2 $\times 10^{-3}$
0.005	2	1.964	2.585	3.24	5.0
0.01	3	1.175	1.723	1.239	2.2
0.05	15	0.294	0.344	0.107	0.088
0.1	29	0.144	0.178	0.023	0.023

2. Finite temperature and bias voltage

Finally, let us consider both finite temperature and bias voltage. This case corresponds to the regime considered in subsection II B 2. There, an effective number of resonances was introduced, Eq. (14), which corresponds to the number of autoconvolutions of the distribution $p(g)$, Eq. (9), to be used in order to obtain $P(G(T, V))$. In Fig. 7 we present the results for $P(G(T, V))$ (histograms in solid line) from the convolution method for $L = 400$, $V = 0.01$, and four different values of T . For each value of T , the number of convolutions N_{eff} changes according to Eq. (14). As in previous cases, we compare to the numerical simulations (histograms in dashed line). A good agreement is seen in all cases.

The first moments of the conductance distribution were also obtained. The results are shown in Table II, where, as before, Σ_q is obtained from the numerical simulation, while σ_q is computed from the expression for $p(g)$, Eq. (9). The agreement between the numerical simulation and theory is, in general, reasonably good. We recall that at finite T we have introduced the simplification of representing the difference of the Fermi functions by a rectangular function, Eq. (13). This additional approximation might be the cause for the discrepancies between Σ_q and σ_q/N_{eff}^{q-1} observed for small values of N_{eff} (first two lines of table II). Notice that a small error in the estimate of the integer number N_{eff} implies a large relative error for small N_{eff} . In all cases, however, the behavior of the moments and the conductance distribution is well described by our method.

Finally, it worth mentioning that we have verified that the approach based in convolutions of $p(g)$ also provides a good approximation to the exact $P(G(T, V))$ at finite

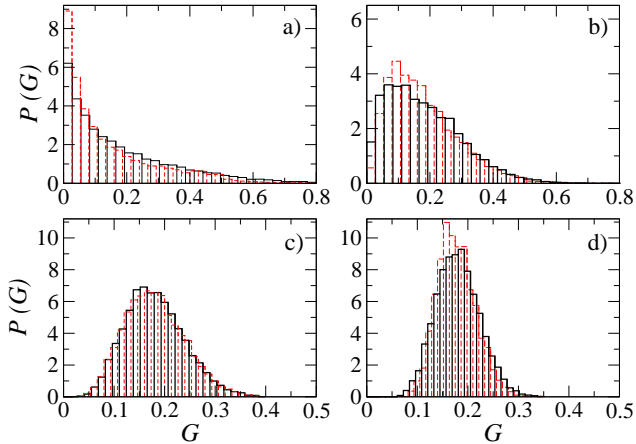


FIG. 7: (Color online) Numerical distributions $P(G)$ (dashed red line histograms) of a system with length $L = 400$, $V = 0.01$, and different temperatures: a) $T = 0.005$, b) $T = 0.01$, c) $T = 0.05$, d) $T = 0.1$. The theoretical distribution from N_{eff} autoconvolutions of $p(g)$ (solid line histograms) are compared with the corresponding numerical results: a) $N_{eff} = 2$, b) $N_{eff} = 3$, c) $N_{eff} = 15$, d) $N_{eff} = 29$. A good agreement is observed.

T in cases with larger eV (e.g. $eV = 0.1, 0.2$).

IV. SUMMARY AND CONCLUSIONS

In an independent electron picture and assuming full phase-coherent electronic transport, we have studied the distribution of the conductance $P(G(T, V))$ in 1D-disordered systems at finite temperature and bias voltage.

We have observed a strong effect of finite T and V at the level of the conductance distribution. In general $P(G(T, V))$ is narrower compared to the conductance distribution at $T = 0, V \sim 0$. The average of the conductance is, however, independent of T and V (see Fig. 2). This implies that higher moments have to be analyzed to see the effect of the temperature and voltage.

When temperatures and voltages are small (less than the mean-level spacing), only one resonance is relevant to the conductance. In this regime, the distribution of the conductance is well described by a simplified resonant-

tunneling model, Eq. (5), as we have verified numerically. As the temperature and bias voltage is increased several resonances contribute to $G(T, V)$. In this regime, the conductance distribution $P(G(T, V))$ can be obtained from the convolutions of the known distribution of conductance at zero temperature and bias voltage $p(g)$. The number of autoconvolutions of $p(g)$ is determined by the width of the energy window where transport can take place. In the case of zero temperature and finite bias voltage, the width of the energy window is trivially eV and the number of convolutions is given by the mean number of levels $N = eV/\Delta$. In the case of finite temperature and a finite bias voltage, we have simplified the problem by introducing an effective number of resonances that allow us to reduce the problem of finite T and V to the simpler case of zero temperature, and finite V . The results of our theoretical method have been compared to numerical simulations of a 1D-disordered system at different regimes of temperature, voltage, and different values of the length of the system. A good agreement has been found in all cases. We point out that for small T and V the line shape of the resonances was relevant in the calculation of $G(T, V)$ (see Section II A). When the values of T and V are such that several resonances contribute to the conductance, the line shape is seen to be irrelevant. To conclude, we remark that with the resonant model and the convolution method of sections II A and II B, respectively, we are able to analyze the conductance distribution at all regimes of temperature and bias voltage, under the assumptions described in the paper.

V. ACKNOWLEDGMENTS

F. F is grateful to the hospitality of BIFI in Zaragoza and CAB in Bariloche where part of this work has been done, and to AUIP for a travel grant. M.J.S. and L.A. acknowledge financial support from PICT 0311609 and (M.J.S.) from Fundación Antorchas and PICT 0313829 from ANPCyT, Argentina. L. A. and V. A. G. also acknowledge financial support from the Ministerio de Educación y Ciencia, Spain, through the Ramón y Cajal Program. This work was supported by grant “Grupo de investigación de excelencia DGA” and (L.A.) BFM2003-08532-C02-01 from MCEyC of Spain. L.A and M.J.S. are staff members and F.F is fellow of CONICET, Argentina.

¹ N. Agrait, A. L. Yeyati, and J. M. van Ruitenbeek, Phys. Rep. **377**, 81 (2003).
² R. Saito, *Physical properties of carbon nanotubes*, Imperial College Press, London (1998).
³ C. Weisbuch and B. Vinter, *Quantum Semiconductor Structures: Fundamentals and Applications*, Academic Press (1991).
⁴ R. Schäfer, K. Hecker, and H. Hegger, Phys. Rev. B **53**,

15964 (1996).
⁵ R. Häussler, H. B. Weber and H. v. Löhneysen, J. of Low Temperature Physics **118**, 467 (2000).
⁶ C. Terrier, D. Babic, C. Strunk, T. Nussbaumer, and C. Schönberger, Europhys. Lett. **59**, 437 (2002).
⁷ P. A. Mello and N. Kumar, *Quantum Transport in Mesoscopic Systems. Complexity and statistical fluctuations*, Oxford University Press, Oxford, (2004).

- ⁸ C. W. J. Beenakker, Rev. Mod. Phys. **69**, 731 (1997) and references therein.
- ⁹ M. Ya Azbel and D.P. Di Vincenzo, Phys. Rev. B. **30**, 6877 (1984).
- ¹⁰ M. Moško, P. Vagner, M. Bajdich, and T. Schäpers, Phys. Rev. Lett. **91**, 136803 (2003).
- ¹¹ Victor A. Gopar and Peter Wöelfle, Europhys. Lett. **71**, 966 (2005).
- ¹² N.F. Mott *Metal-Insulator Transitions* Taylor & Francis, U.K. (1990)
- ¹³ A. D. Stone and P.A. Lee, Phys. Rev. Lett. **54** 1196, (1985).
- ¹⁴ R. A. Serota, R. K. Kalia and P. A. Lee, Phys. Rev. B, **33**, 8441, (1986).
- ¹⁵ P. F. Bagwell and T. P. Orlando, Phys. Rev. B **40**, 1456 (1989).
- ¹⁶ E.R. Mucciolo, R.A. Jalabert and J-L. Pichard, J. Phys. (France) **7**, 1267 (1997)
- ¹⁷ C. W. J. Beenakker and B. Rejaei, Phys. Rev. Lett. **71** 3689 (1993).
- ¹⁸ S. Datta, *Electronic Transport in Mesoscopic Systems*, Cambridge University Press, Cambridge, U.K. (1995).